

Modulation of Magnetic Anisotropy and Exchange Interaction in Phenoxide-Bridged Dinuclear Co(II) Complexes

Ajit Kumar Kharwar,[§] Arpan Mondal,[§] Arup Sarkar, Gopalan Rajaraman,* and Sanjit Konar*

Cite This: *Inorg. Chem.* 2021, 60, 11948–11956

Read Online

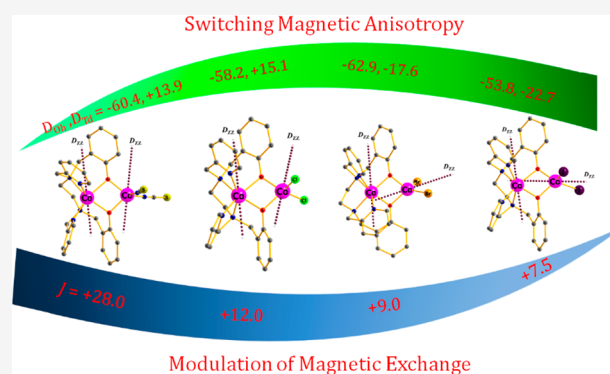
ACCESS |

Metrics & More

Article Recommendations

Supporting Information

ABSTRACT: We report a new class of four dimeric Co(II) complexes [Co₂(bbpen)(X)₂] (H₂bbpen = *N,N'*-bis(2-hydroxybenzyl)-*N,N'*-bis(2-methylpyridyl)ethylenediamine) [X[−] = SCN[−] (1), Cl[−] (2), Br[−] (3), and I[−] (4)] with different coordination geometry of two Co(II) centers (trigonal-prismatic and pseudo-tetrahedral) and their magnetic study. Interestingly, the two Co(II) centers show two different types of magnetic anisotropy. State of the art ab initio CASSCF analysis reveals that the six-coordinate or the trigonal-prismatic Co(II) center possesses a consistently large negative axial zero-field splitting (negative *D*) parameter (~ -60 cm^{−1}), while the four-coordinate or the pseudo-tetrahedral Co(II) center exhibits a range of *D* values from +13 to -23 cm^{−1}. Ab initio calculations employing the lines model were used to estimate the magnetic exchange as both the Co(II) centers possess significant magnetic anisotropy. All the complexes display rare ferromagnetic interaction, and the strength of this interaction decreases as the ligand field on the pseudo-tetrahedral Co(II) center decreases from SCN[−] > Cl[−] > Br[−] > I[−].



INTRODUCTION

The phenomenon of magnetic exchange is highly important in the field of single-molecule magnets (excluding single-ion magnets (SIMs)) and magnetically coupled metal–organic frameworks (MOFs) as it controls the overall magnetic behavior of these complexes.¹ Magnetic exchange coupling can fairly reduce quantum tunneling of magnetization between the ground states and can force relaxations to occur through the thermal paths.² This can significantly enhance the energy barrier of the relaxation pathways in magnetically coupled polymetallic complexes.² Applications of these polymetallic complexes in the field of information storage, spintronics, low-temperature magnetic refrigeration, and quantum computing make them a material of great interest.³

Magnetic exchange of these systems largely depends on factors like type of bridging ligand (oxo, phenoxo, azide, carboxylates, dicynamato, and cyanide), metal–ligand bond length, dihedral angles between the coordination planes, torsion angles, bond angles created by bridging atoms, and so on.^{3,4} Binuclear or trinuclear units are the most basic structural unit for polymetallic complexes.⁴

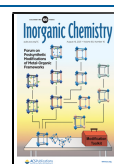
Thus, understanding and exploration of the relationship between magnetic exchange and structure of those basic units (magneto-structural correlation) can provide a platform for probing and modulating the magnetic property of polymetallic complexes.^{4,5}

The anomalous paramagnetic behavior of “monomeric” copper acetate was the elementary work in this field. The

magnetic property was explained by dimeric molecular structure of copper acetate as obtained from single-crystal X-ray diffraction.^{6,7} Thereafter, many dinuclear complexes of first-row transition metal ions such as Fe(III),⁸ Cr(II) and Cr(III),⁹ Mn(II) and Mn(III),¹⁰ and Ni(II)¹¹ have been reported, and their magneto-structural correlations have been studied. The theoretical approach to support the experimental observation has become an important tool that can provide detailed mechanism of the magnetic exchange (*J*) and electronic structure of these complexes.^{12,13} For example, DFT calculations were used by Berg et al. to understand the mechanism of magnetic exchange in Mn(III) dimers.^{4b} On the other hand, understanding of exchange mechanism for an anisotropic system is complicated as it is very difficult to separate the exchange coupling constant and anisotropic parameters.¹⁴ Therefore, tuning of exchange coupling (especially ferromagnetic interaction) with the anisotropy is one of the most challenging tasks in the field of molecular magnetism as both have a significant impact on slow magnetic relaxation.¹⁵ In this regard, Co(II) has emerged as a promising

Received: March 28, 2021

Published: July 27, 2021



candidate for the synthesis of the single-molecule magnets (SMMs) due to its giant magnetic anisotropy and resilient ZFS parameter.^{16,17}

Numerous Co(II) dinuclear complexes have been explored to understand the magnetic anisotropy and exchange interactions.¹⁸ But in most of them, both the cobalt centers had the same coordination environment with less distortion around the metal centers from ideal geometries (e.g., O_h) and show antiferromagnetic exchange interaction.¹⁸ In addition, many polymetallic cobalt clusters have been reported where all the cobalt centers are not present in the same geometry, and the magnetic exchange of such systems is unrevealed.¹⁹ In this paper we report a new class of four dimeric Co(II) complexes $[Co_2(bbpen)(X)_2]$ ($H_2bbpen = N,N'$ -bis(2-hydroxybenzyl)- N,N' -bis(2-methylpyridyl)ethylenediamine) [$X = SCN^-$ (1), Cl^- (2), Br^- (3), and I^- (4)] with two different coordination geometry of Co(II) centers (trigonal-prismatic and pseudo-tetrahedral). Magnetic studies and ab initio calculations reveal the presence of ferromagnetic exchange interactions between the two metal centers, which can be tuned by varying the terminal ligands from pseudo-halide SCN^- to halides Cl^- , Br^- , and I^- . In addition, the switching of magnetic anisotropy was also observed with the changing of ligand field for the four-coordinate Co(II) center. Therefore, for the first time we report tuning of both ferromagnetic exchange interaction and anisotropy parameters in dinuclear Co(II) complexes, where Co(II) centers are coordinated in two different ligand environments.

RESULTS AND DISCUSSION

Crystallography. Complex 1 crystallizes in monoclinic $P2_1/n$ space group with asymmetric unit composed of one dinuclear complex and one acetonitrile molecule (for detailed information see Table S1). The single unit of ligand $bbpen^{2-}$ binds in a κ^6 fashion to Co1 and in a κ^2 fashion to Co2, whereas the other two coordination sites of the Co2 are occupied by pseudo-halide SCN^- and halides X^- (Cl, Br, and I) (Figures 1 and 2). In the dinuclear unit, the two cobalt centers are bridged with the μ -phenoxide group of the ligand $bbpen^{2-}$. In the hexacoordinated cobalt center of complex 1,

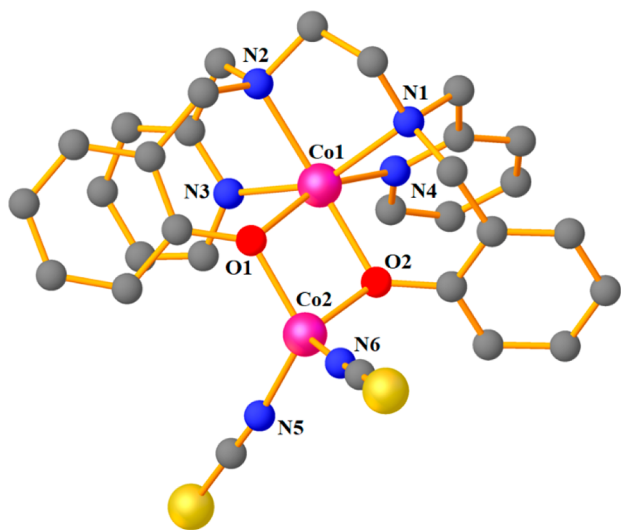


Figure 1. Crystal structure of 1 (asymmetric unit) viewed as a ball-and-stick model. Color codes: pink = Co, red = O, blue = N, and light gray = C (hydrogens are omitted for clarity).

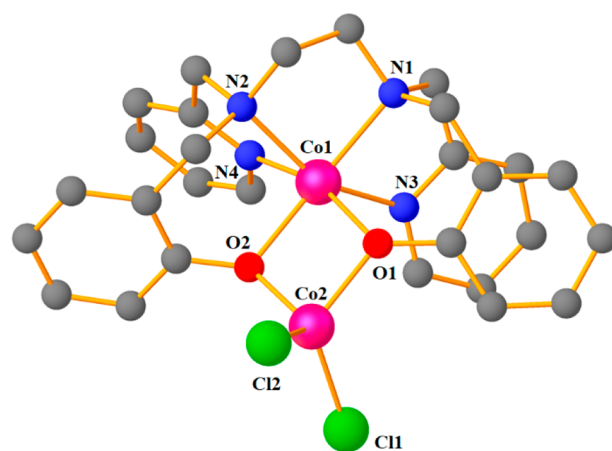


Figure 2. Crystal structure of 2 (asymmetric unit) viewed as a ball-and-stick model. Color codes: pink = Co, red = O, blue = N, light gray = C, and green = chloride (hydrogens are omitted for clarity).

the three trans angles are $\angle N1-Co1-O2 = 156.72^\circ(6)$, $\angle N2-Co1-N3 = 151.00^\circ(7)$, and $\angle O1-Co1-N4 = 159.27^\circ(6)$, represent the distortion around the Co1 metal center from the octahedral geometry (trans angles must be 180° for perfect O_h geometry). The bond angle around the four-coordinate cobalt center in complex 1 is $\angle N6-Co2-N5 = 113.76^\circ(8)$ and for chelated $\angle O1-Co2-O1 = 83.52^\circ(6)$ also signifies the high distortion from the tetrahedral geometry (angles must be 109.5° for perfect T_d geometry).

The continuous shape measurement (CShM)²⁰ revealed that the hexacoordinated and tetraordinated centers have trigonal-prismatic geometry and pseudo-tetrahedral geometry with a deviation factor of 4.347 and 1.869, respectively.

Complexes 2 and 3 crystallize in the triclinic space group $P-1$, and 4 crystallizes in monoclinic space group $C2/c$. Complexes 2–4 have one binuclear unit without any solvent molecule in the asymmetric unit. As complexes 2–4 share many structural features, we have taken complex 2 as representative for complexes 3 and 4 for further narration of the crystal structure. Two molecules are present in the triclinic unit cell of complex 2 (an enantiomeric pair) (Figure S1). Bond lengths and angles relating to the coordination at the metals are given in Table S2. In the hexacoordinated cobalt center of complex 2 the three trans angles are $\angle N1-Co1-O2 = 158.08^\circ(10)$, $\angle N2-Co1-N3 = 152.18^\circ(12)$, and $\angle O1-Co1-N4 = 161.38^\circ(10)$ which represent the very high degree of distortion from octahedral geometry. This is supported by the CShM with the deviation factor of 4.752, which is zero for perfect O_h geometry. A complete result of geometric analysis is shown in Table S3.

In complex 2 the second cobalt center (four-coordinate) is also highly distorted from the ideal T_d geometry (like the previously reported Zn analogue complex⁴⁸) as confirmed by the CShM with a deviation factor of 2.655. The $\angle Cl1-Co2-Cl2$ bond angle is $113.92^\circ(5)$, and for chelated $\angle O1-Co2-O2$ the bond angle is $83.39^\circ(10)$. The $Co2-O1$ and $Co2-O2$ bond lengths are shorter than the $Co2-Cl1$ and $Co2-Cl2$ bonds, introducing further asymmetry to the four-coordinate Co(II) site. Shape analyses reveal trigonal-prismatic and pseudo-tetrahedral geometries around six- and four-coordinate cobalt centers in complexes 3 and 4, respectively (a detailed shape analysis is given in Tables S3 and S4).

In all the complexes the pyridine rings and the phenoxide-functionalized benzene rings of bbpen^{2-} have intramolecular $\pi\cdots\pi$ interactions, and in complex 2 the distances between the π -rings are 3.605 and 3.962 Å, as shown in Figure S2. For other complexes, the $\pi\cdots\pi$ stacking details are given in Table S5. All the complexes have strong $\text{CH}\cdots\pi$ interactions between the π_{phen} of one asymmetric unit of the complex with hydrogens (H from CH_2 of ethylenediamine) of another asymmetric unit to form a dimeric structure (Figure S3). For complex 1 the $\text{CH}\cdots\pi$ distance is 2.697 Å, and for complexes 2, 3, and 4 it is 2.739, 2.617, and 2.679 Å, respectively. Two chlorides in one unit of complex 2 are in $\text{H}\cdots\text{Cl}$ interaction with the four neighboring dinuclear units of the complex 2 (Figure S4), and the pattern is further extended to form a strong 3D packed structure (Figure S5). The average of $\text{H}\cdots\text{Cl}$ interaction (H-bonding) is 3.124 Å in complex 2; however, in complexes 3 and 4 it is 3.257 Å ($\text{H}\cdots\text{Br}$ interaction) and 3.355 Å ($\text{H}\cdots\text{I}$ interaction), respectively.

Magnetic Characterization. The temperature dependence of direct current (dc) magnetic susceptibility data was measured for all complexes in the temperature range 2–300 K under an applied field of 0.1 T. The phase purity of the bulk samples has been confirmed by good agreement of the powder X-ray diffraction pattern with the simulated one obtained from the single-crystal structure data (Figure S6). The room temperature $\chi_M T$ values (χ_M = molar magnetic susceptibility) were obtained as 6.74, 6.29, 6.18, and 6.05 $\text{cm}^3 \text{mol}^{-1} \text{K}$ for complexes 1–4, respectively (Figures 3 and 4). For all the

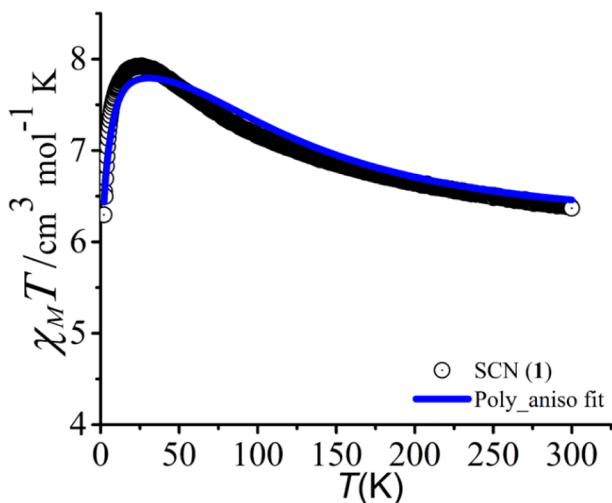


Figure 3. Plot of the $\chi_M T$ vs T for complex 1 in an applied field of 0.1 T.

complexes the $\chi_M T$ values were higher than the spin-only value as expected for two cobalt centers (Co^{II} , $S = 3/2$, $g = 2.0$, and $\chi_M T = 1.87 \text{ cm}^3 \text{mol}^{-1} \text{K}$ for one cobalt center) because of their considerable contribution to the orbital angular momentum.

In all the complexes, upon cooling the temperature from 300 K, the $\chi_M T$ value slowly increases and reaches a maxima, which represents the ferromagnetic interaction between the two cobalt centers. For complex 1 the maximum was observed as 7.96 $\text{cm}^3 \text{mol}^{-1} \text{K}$ at 24 K; on further lowering the temperature it decreases rapidly due to the anisotropic nature of the Co^{II} center and reaches a value of 6.31 $\text{cm}^3 \text{mol}^{-1} \text{K}$ at 2 K. For complexes 2–4, the ferromagnetic interactions lead to the

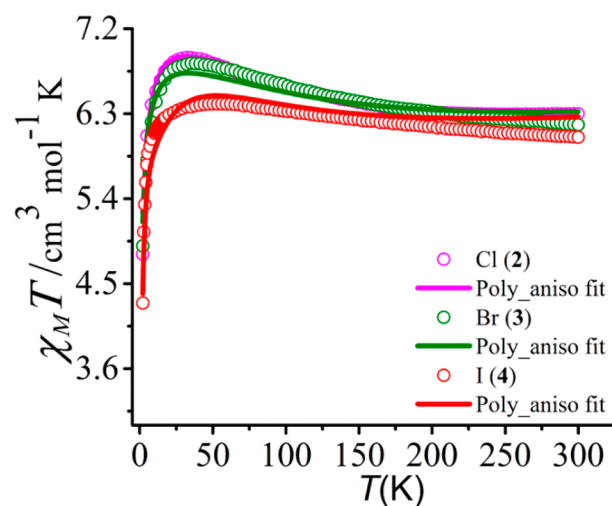


Figure 4. Plot of the $\chi_M T$ vs T for complexes 2–4 in an applied field of 0.1 T.

increase of the $\chi_M T$ value with decreasing temperature, and the maxima reach a value of 6.89 (2), 6.83 (3), and 6.40 $\text{cm}^3 \text{mol}^{-1} \text{K}$ (4) at different temperatures 32 (2), 33 (3), and 40 K (4), respectively. In addition, lowering the temperature, the $\chi_M T$ value sharply decreases to 4.8 (2), 4.9 (3), and 4.2 $\text{cm}^3 \text{mol}^{-1} \text{K}$ (4) at 2 K and indicates the presence of significant magnetic anisotropy in all the complexes. On the other hand, it was also observed that the strength of the ferromagnetic exchange interaction between two cobalt centers gradually decreases from complexes 1–4 as the extent of increase as well as the peak maxima of $\chi_M T$ value decreases in the same order. This is probably due to the different ligand field strength around the Td Co^{II} centers, which may result in different d-orbital splitting and overlap integral between two cobalt centers which controls the overall exchange interaction in the studied compounds. We have measured the field dependence of magnetization for all complexes in the range of field 0–7 T at different temperatures of 2, 4, and 6 K. The M vs H (Figure 5 and Figure S7a–c) isotherms show that the magnetization value did not reach saturation at 2 K even at 7 T. Probably, the highest available field (7 T) may not be sufficient to fully populate the excited

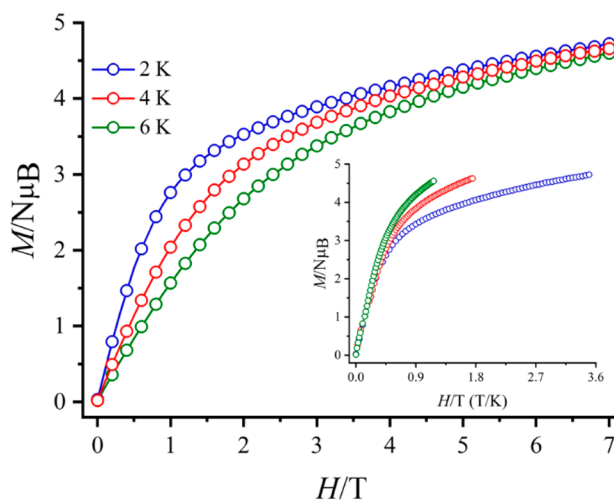


Figure 5. $M/N\mu_B$ vs H plot for complex 1 at the indicated temperatures (inset: reduced magnetization plot).

Table 1. CASSCF Computed Spin-Hamiltonian Parameters of the Four Complexes

complex	D_{O_h} (cm^{-1})	D_{T_d} (cm^{-1})	E/D_{O_h} , E/D_{T_d}	g_x , g_y , g_z (O_h)	g_x , g_y , g_z (T_d)
1	-60.4	13.9	0.11, 0.23	2.09, 2.21, 2.84	2.41, 2.32, 2.21
2	-58.2	15.1	0.12, 0.32	2.09, 2.21, 2.82	2.53, 2.40, 2.28
3	-62.9	-17.6	0.13, 0.10	2.07, 2.21, 2.86	2.32, 2.38, 2.58
4	-53.8	-22.7	0.09, 0.06	2.11, 2.20, 2.77	2.32, 2.39, 2.65

states to reach magnetization saturation for the studied complexes. In addition, it was observed that the highest magnetization values are in the range 4.70–5.32 μ_B for complexes 1–4 which are relatively lower than the expected value (6.6 and $g = 2.2$ for two cobalt) as the plateau has not been reached in the magnetization plot at 7 T. The nonsuperimposable nature of the reduced magnetization plot M vs H/T for 1–4 also signified the presence of high anisotropy in all complexes (Figure 5 and Figure S7a–c).

Considering the dinuclear structure of all the complexes, we performed the fitting with PHI²¹ software to quantify the exchange coupling parameter (J_{ex}). However, no good fit was obtained with the acceptable parameters (2–300 K) for complexes 1–4. There are reports of some relevant phenoxide-bridged Co(II)-based dinuclear complexes.²² For example, Massoud et al. reported an antiferromagnetically coupled Co(II)-based dinuclear complex where both the metal centers are present in distorted O_h geometry.^{22e} A fitting procedure of the susceptibility data resulted in an exchange value of -8.38 cm^{-1} with a zero-field splitting (ZFS) parameter (D) of 25.7 cm^{-1} and $g = 2.39$. The results confirmed the moderate antiferromagnetic exchange between Co(II) atoms and the substantial role of magnetic anisotropy as deduced from the axial ZFS parameter. Similarly, Lin et al. also reported a phenoxide-bridged bicobalt complex with an octahedral geometry of both metal Co(II) atoms.^{22f} The experimental magnetic data were analyzed by Lines' model which leads to the exchange value (J) -4.22 cm^{-1} . So the reported phenoxide-bridged Co(II)-based dinuclear complexes have a single anisotropy parameter due to the same geometry and ligand field around the metal centers. At the same time, the two Co(II) centers of the dinuclear complexes reported in this work have different symmetry which leads to different types of magnetic anisotropy. Thus, it is more difficult to fit (both the susceptibility and magnetization data) and extract the anisotropic parameters as well as exchange coupling constant for the studied complexes. To understand the anisotropy of the system, we have performed *ab initio* calculations (*vide infra*) individually for two cobalt centers in all the complexes. The concurrent simulation of both the dc magnetic susceptibility and magnetization data using the poly_aniso program reveals the presence of ferromagnetic interaction between the cobalt centers, which decreases from complexes 1–4. In addition, the presence of easy-axis anisotropy has been observed in six-coordinate Co(II) centers, whereas four-coordinate Co(II) centers possess two types of magnetic anisotropy (easy-plane anisotropy for 1 and 2, easy-axis anisotropy for 3 and 4) which are also consistent with reported complexes.

In addition, the alternating current (ac) susceptibility measurements were performed to check the relaxation dynamics of the studied complexes (for 1 and 4). However, no out-of-phase ac signals were observed, which may be due to the strong intermolecular interaction and shorter Co–Co distances (Table S6) leading to the faster relaxation through

QTM, spin–spin, or spin–lattice relaxation process in these dinuclear compounds (Figure S8a,b).^{22g}

Theoretical Studies. Molecules 1–4 have a different source of anisotropy which is difficult to extract. The octahedral Co(II) ions are expected to have unquenched orbital contribution arising from the ground state, while the four-coordinate Co(II) is known to yield very large anisotropy due to out-of-state contributions. Additionally, as they are bridged by the oxo group, the exchange coupling between the two metals is expected to be significant, complicating the magnetic properties of these simple dinuclear systems. To extract the relevant spin-Hamiltonian parameters on the local paramagnetic centers (see the Computational Details section), independently, we have decided to perform *ab initio* calculations on 1–4 (X-ray structures) based on multi-configurational CASSCF methods which are known to yield a good numerical estimate of the single-ion anisotropy (see Table 1). Hence, during these calculations one of the Co(II) centers was replaced by a diamagnetic Zn(II) ion. We have also performed calculations on DFT-optimized geometries, but these tend to alter the ZFS of tetrahedral Co(II) center significantly (see the Supporting Information and Table S7 for details).²³ Furthermore, computationally expensive NEVPT2 calculations have been performed on the four complexes to confirm the sign of D values obtained from the CASSCF method (see Table S8). NEVPT2 correction of the ZFS parameters slightly reduces the magnitude of D on the octahedral sites; however, on the tetrahedral sites, it remains the same. For the *ab initio* treatment of exchange coupling and wave function analysis, we have restricted ourselves to the less expensive CASSCF level of theory.

The calculated values suggest that all the hexacoordinated Co(II) centers show negative or easy-axis anisotropy with a D value around -60 cm^{-1} . Easy-axis anisotropy in six-coordinate Co(II) complexes with a small rhombic anisotropy (low E/D or $E/D < 0.2$) suggests a trigonal-prismatic or antiprismatic (TRP) geometry around the Co(II) center with the anisotropy axis along the trigonal or C_3 -axis.²⁴ Indeed, the EHA (effective Hamiltonian approach) computed D_{zz} axes of all six-coordinate Co(II) centers in 1–4 are aligned along the pseudo- C_3 -axis of the molecules (see Figure S9).

The negative D in the case of TRP geometry for Co(II) species can also be rationalized from its CASSCF-LFT d-orbital splitting diagram (shown in Figure 6). The first excited state, which arises from the dominant same M_L valued $d_{x^2-y^2}$ to d_{xy} electronic transition, contributes significantly to the negative D value estimated. This is confirmed from the multiconfigurational wave function analysis (see Table S9).²⁵ While all the six-coordinate Co(II) centers yield very similar D values, there is some difference among these values, and these are due to small structural changes associated with complexes 1–4. Particularly the ground state to excited state gap directly correlates to the magnitude of the D value computed with complex 3 possessing the smallest gap and complex 4 possessing the largest gap (see Table S10).

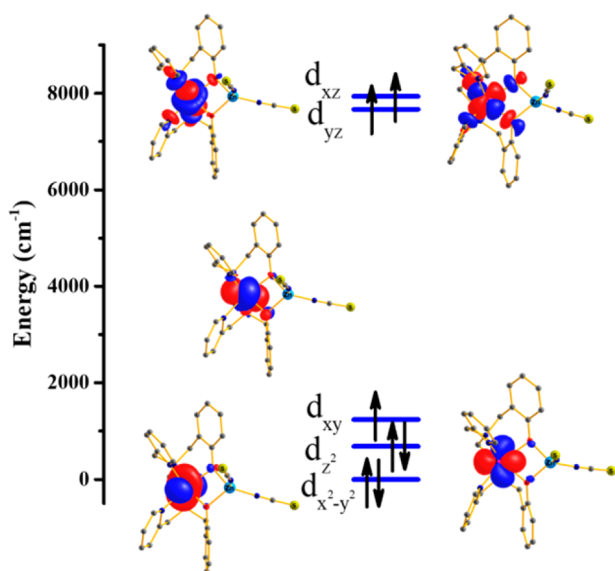


Figure 6. CASSCF-LFT splitting diagram at the six-coordinate Co(II) site for complex 1.

While the six-coordinate Co(II) centers in all four complexes show consistent negative D parameters, four-coordinate Co(II) centers show a drastic change in the D values ranging from $+14 \text{ cm}^{-1}$ in complex 1 to -23 cm^{-1} in complex 4. Unlike six-coordinate Co(II), here the D_{zz} orientation switches its direction from complexes 1 and 2 to complexes 3 and 4 when the sign of D also switches from positive to negative D values (see Figure S9). This switching in the sign of D_{T_d} and in orientation is reflected in a high E/D value of complex 2, where the D_{T_d} remains in the borderline region.

This observation can be rationalized by careful analysis of the tetrahedral site d-orbital splitting diagram shown in Figure 7. This variation in D_{T_d} is expected as the ligand field strength

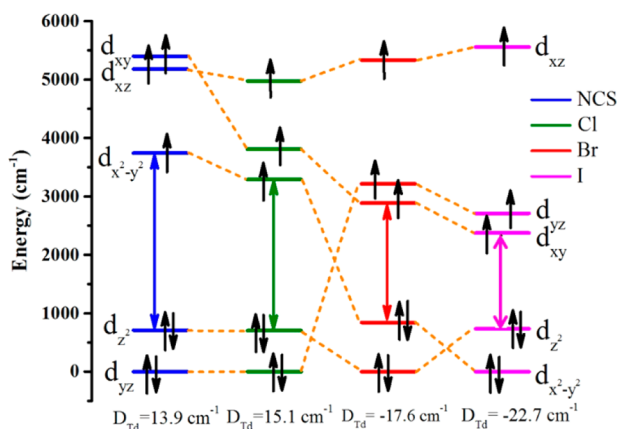


Figure 7. CASSCF ligand splitting diagram of pseudo-tetrahedral Co(II) centers of the four complexes.

decreases from $\text{SCN} > \text{Cl} > \text{Br} > \text{I}$. The orbital splitting pattern also drastically changes as we go from Cl^- to Br^- . The first four excited electronic states primarily contribute to the overall D values of these four-coordinate Co(II) centers. Out of these, in complexes 1 and 2, the major contribution toward positive D_{T_d} arises due to the spin-orbit coupling from the first excited state which is 2894 and 2110 cm^{-1} apart from the ground state

for complexes 1 and 2, respectively (see Tables S11 and S12). This electronic excitation dominantly contributes toward this positive D_{T_d} corresponds to dominant different M_L level $d_{yz} \rightarrow d_{x^2-y^2}$ transition. On the other hand, in complexes 3 and 4 negative D_{T_d} appears due to the SOC with the dominating first excited state contributions which are 1890 and 1602 cm^{-1} , respectively, destabilized from the ground electronic state. The first excited state here is due to the dominant $d_{x^2-y^2} \rightarrow d_{xy}$ same M_L level electronic excitation (see Table S13). Thus, a heavier atom substitution at the tetrahedral Co(II) center leads to negative D value, and this phenomenon is noted earlier in tetrahedral Co(II) complexes.²⁶ Although the bond angle of $\angle X-\text{Co}-X$ ($X = \text{SCN}, \text{Cl}, \text{Br}, \text{and I}$) remains almost the same in the four complexes 1–4, which are in the 113° – 115° range, the Co–X bond length increases from 1.95 Å in complex 1 to 2.60 Å in complex 4 due to the decrease of the donor strength. This trigger change in ALLFT d-orbital splitting pattern and change in both sign and magnitude in D_{T_d} values.^{24h,25,26}

Next, we switched our attention to describe the nature of the magnetic exchange between the two Co(II) centers. From the anisotropic studies reported above, it is clear that both the Co(II) centers have significant ZFS, especially six-coordinate centers where the energy gap between the ground and first excited state Kramers doublets (KDs) is close to 100 cm^{-1} . This large ZFS gap suggests that an isotropic description of exchange Hamiltonian extracted from density functional methods would be inappropriate in these complexes. Therefore, we have extracted the J values using the lines model using the POLY_ANISO routine.²⁷ In this method, the anisotropic exchange interaction between the metal sites is calculated with an isotropic description in the sense that the effective Hamiltonian is calculated on the basis of products of the wave functions corresponds to the chosen low-lying Kramers levels (of each of the Co centers).

Thus, we have computed the exchange coupling along with the SINGLE_ANISO values considering the lines (Heisenberg + Ising) model using the spin-Hamiltonian

$$\begin{aligned} \hat{H} = & D_{O_h} \left[\hat{S}_z^2 - \frac{1}{3} S(S+1) \right] + E_{O_h} (\hat{S}_x^2 - \hat{S}_y^2) \\ & + D_{T_d} \left[\hat{S}_z^2 - \frac{1}{3} S(S+1) \right] + E_{T_d} (\hat{S}_x^2 - \hat{S}_y^2) \\ & - J_{\text{tot}} \hat{S}_{O_h} \cdot \hat{S}_{T_d} + zJ' \end{aligned}$$

Here, \vec{J}_{tot} represents the complete tensor of the exchange interaction between the two Co(II) centers. The full exchange Hamiltonian contains the (an)isotropic exchange part, the antisymmetric exchange (Dzialoshinski–Moriya interaction) term, and the dipolar interaction term. Here, because of the presence of pseudo- C_{2v} symmetry of the complexes, the antisymmetric exchange is neglected. Pseudo-spins \tilde{S}_1 and \tilde{S}_2 were allowed to couple to generate the final exchange-coupled states. The last term represents the intermolecular exchange term (zJ') which was used to obtain a reasonable fit of χT at a very low temperature.

The SINGLE_ANISO computed D values for both the anisotropic centers and POLY_ANISO fitted exchange parameters on the X-ray structures have been tabulated in Table 2. During the POLY_ANISO fit, we have only varied the exchange coupling parameter J_{ex} ($J_{\text{tot}} = J_{\text{ex}} + J_{\text{dip}}$); all other parameters like D , E , g_x , g_y , and g_z values were fixed from

Table 2. CASSCF-RASSI-SO_SINGLE_ANISO Computed Local ZFS Parameters on the Four Complexes and POLY_ANISO Computed Coupling Interactions (g -Factors Have Been Taken from Table 1)

complex	CASSCF $D(O_h)$ (cm^{-1})	CASSCF $D(T_d)$ (cm^{-1})	$J_{\text{tot}} = J_{\text{ex}} + J_{\text{dip}}$ (cm^{-1})	zJ (cm^{-1})
1	−61.1	13.9	28.0	−0.01
2	−59.3	15.3	12.0	−0.02
3	−64.1	−18.0	9.0	−0.07
4	−55.5	−23.0	7.5	−0.08

SINGLE_ANISO calculations. Dipolar contributions expected due to the asymmetry of the Co(II) centers were found to be very small ($<0.1 \text{ cm}^{-1}$) for all the complexes. The POLY_ANISO fit shows a nice agreement with the experimental χT vs T and M vs H curves for all the complexes (Figures 3 and 4, Figure S10). The fit yields a ferromagnetic coupling between two Co(II) centers; the computed CASSCF orbitals for both centers also suggest significant orbital orthogonality as the one center Co(II) ion is in six-coordination with the unpaired electron remaining in d_{xy} , d_{xz} , and d_{yz} orbitals while in the other four-coordinate Co(II) ion they remain in $d_{x^2-y^2}$, d_{xz} , and d_{xy} (for complex 1) orbitals. The low-lying exchanged coupled spin–orbit states of the four complexes are shown in Figure S11. The tunnel splitting values for all the complexes for the ground state non-Kramers pairs is significantly high (>0.4), which eliminates the possibility of observance of zero/dc field ac signals in all the complexes.

The orbital plots shown in Figures 6 and 7 reveal that the possible overlap that could contribute to antiferromagnetic coupling is $d_{xz}|d_{xz}$ overlap while all other SOMOs are expected to have very little overlap or orthogonal leading to moderate ferromagnetic coupling. The J_{tot} value shows a very high ferromagnetic coupling of 28 cm^{-1} in the case of complex 1, while it decreases to less than half at complex 2 in 12 cm^{-1} and then decreases slightly at 9 and 7.5 cm^{-1} for complexes 3 and 4, respectively. As the Co–O–Co angle remains similar for complexes 1–4, the difference in coupling estimated is due to the variation in the orbital occupation. As we move from complex 1 to complex 4, the orbital ordering in the tetrahedral Co(II) site alters offering a possible $d_{yz}|d_{yz}$ overlap on top of the existing $d_{xz}|d_{xz}$ overlap, enhancing the antiferromagnetic contribution to the J and hence decreasing the net ferromagnetic coupling observed. In addition to the exchange contribution to the net J values, the dipolar contribution exists, and this is correlated to the distance and the orientation of the major magnetic anisotropy axes. Significantly enough, the D_{zz} and g_{zz} axis of the tetrahedral Co(II) ions for complexes 1–4 are tilted with respect to each other. For complex 1, the D_{zz} axes of both Co(II) ions are nearly collinear while they are nearly perpendicular to each other in complex 4 (see Figure S9). These differences reveal variation in the dipolar contributions which are reflected in the estimated J values.

CONCLUSION

In this study, we report ferromagnetic exchange interaction in four Co(II) dinuclear complexes of general formulas $[\text{Co}_2(\text{bbpen})(\text{X})_2]$ ($\text{H}_2\text{bbpen} = N,N'$ -bis(2-hydroxybenzyl)- N,N' -bis(2-methylpyridyl)ethylenediamine) [$\text{X} = \text{SCN}^-$ (1), Cl^- (2), Br^- (3), and I^- (4)] with two different (hexa and tetra)coordination environment. Magnetic measurements and ab initio calculations disclose easy-axis anisotropy for six-

coordinate geometry in all complexes whereas a switching of anisotropy from easy plane (1 and 2) to easy-axis (3 and 4) was observed for the four-coordinate cobalt center. Further the extent of ferromagnetic interaction decreases from complexes 1–4. The ligand field strength of the terminal ligands on the four-coordinate cobalt center mainly control the d orbital energy splitting which further plays a pivotal role in switching of anisotropy as well as in the extent of ferromagnetic interaction as observed for complexes 1–4. Notably, this work represents the first example of Co(II) dinuclear complexes, where Co(II) centers are coordinated in two different ligand environments. Moreover, a change in the ligand donor strength not only has the ability to alter the magnetic anisotropy but also the exchange coupling operating between two Co(II) centers. Finally, this work opens a new window to design highly anisotropic dinuclear Co(II) systems with ferromagnetic exchange interaction which can improve the single molecule magnet behavior.

EXPERIMENTAL SECTION

Materials and Methods. Magnetic measurements were performed by using a Quantum Design SQUID-VSM magnetometer. The measured values were corrected for the experimentally measured contribution of the sample holder, whereas the derived susceptibilities were corrected for the diamagnetic contribution of the sample, estimated from Pascal's tables.²⁸ Elemental analysis was performed with an Elementar Microvario Cube elemental analyzer. IR spectra were recorded in KBr pellets with a PerkinElmer spectrometer. Powder X-ray diffraction (PXRD) data were collected with a PANalytical EMPYREAN instrument using Cu $K\alpha$ radiation.

Experimental Details. Intensity data were collected on a Bruker APEX-II D8 venture diffractometer by using graphite monochromated Mo $K\alpha$ radiation ($\lambda = 0.71073 \text{ \AA}$) at 140 K. Data collections were performed by using φ and ω scans. Olex2²⁹ was used as the graphical interface, and the structures were solved with the ShelXT³⁰ structure solution program using intrinsic phasing. The models were refined with ShelXL³⁰ with full matrix least-squares minimization on F^2 . All non-hydrogen atoms were refined anisotropically. Crystallographic data for complex 1 have been summarized in Table S1. Bond lengths and angles are listed in Tables S14 and S15.

Synthesis of Ligand. The ligand (H_2L) was synthesized according to the reported literature.³¹

Synthesis of 1. The ligand H_2L (0.1 mmol, 45.6 mg) was dissolved in 5 mL of dichloromethane, and triethylamine solution (0.2 mmol, 20.22 mg) was added with constant stirring; after 5 min $\text{Co}(\text{SCN})_2$ (0.2 mmol, 35 mg) was added, and the reaction mixture was heated for the next 2 h at 60°C . After that, the reaction mixture was filtered out, and the precipitate was dissolved again in fresh acetonitrile. Good quality crystals suitable for SC-XRD were obtained by the vapor diffusion of diethyl ether to the saturated solution of precipitate in acetonitrile. Yield 56%. Elemental analysis data for 1 were calculated for $\text{C}_{32}\text{H}_{31}\text{Co}_2\text{N}_7\text{O}_2\text{S}_2$: C, 52.82; H, 4.29; N, 13.48; S, 8.81%. Found: C, 52.45; H, 4.21; N, 13.38; S, 8.88%.

Synthesis of 2. The ligand H_2L (0.1 mmol, 45.6 mg) was dissolved in 5 mL of dichloromethane, and triethylamine solution (0.2 mmol, 20.22 mg) was added with constant stirring; after 5 min $\text{CoCl}_2 \cdot 6\text{H}_2\text{O}$ (0.2 mmol, 47.8 mg) was added, and the reaction mixture was heated for the next 2 h at 60°C . After that, the reaction mixture was filtered out, and the precipitate was dissolved in hot DMF. Good quality crystals suitable for SC-XRD were obtained by the vapor diffusion of diethyl ether to the saturated solution of precipitate in DMF. Yield 67%. Elemental analysis data for 2 were calculated for $\text{C}_{28}\text{H}_{28}\text{Cl}_2\text{Co}_2\text{N}_4\text{O}_2$: C, 52.44; H, 4.40; N, 8.74%. Found: C, 52.38; H, 4.36; N, 8.61%.

Synthesis of 3. Complex 3 was prepared by following a similar procedure as described for complex 2 using CoBr_2 (0.2 mmol, 43.6 mg) instead of $\text{Co}(\text{SCN})_2$. Yield 49%. Elemental analysis data for 3

were calculated for $C_{28}H_{28}Br_2Co_2N_4O_2$: C, 46.05; H, 3.87; N, 7.67%. Found: C, 45.90; H, 3.85; N, 7.57%.

Synthesis of 4. Complex 4 was prepared following a similar procedure as was described for complex 2 by using CoI_2 (0.2 mmol, 62.5 mg) instead of $Co(SCN)_2$. Yield 45%. Elemental analysis data for 4 was calculated for $C_{28}H_{28}Co_2I_2N_4O_2$: C, 40.80; H, 3.42; N, 6.80%. Found: C, 40.61; H, 3.41; N, 6.76%.

Computational Details. CASSCF-QDPT-EHA followed by ab initio ligand field theory (AILFT) calculations have been performed in ORCA 4.0.1 program software.³² Scalar relativistic effects have been taken into account during the calculations with the second-order Douglas–Kroll–Hess (DKH) Hamiltonian. The DKH-contracted version of basis sets like DKH-def2-TZVP for Co, Cl, Br, and S; Sapporo-DKH3-TZP-2012 for I; DKH-def2-TZVP(-f) for N and O; and DKH-def2-SVP for rest of the atoms were used during the calculations. During local zero-field splitting calculations, one of the cobalt centers was substituted with a diamagnetic zinc center. In the CASSCF step the seven metal electrons were optimized in five d-orbitals with 10 quartet and 40 doublet roots. NEVPT2 (*N*-electron valence state perturbation theory) calculations were also performed on the top of CASSCF wave function to account for the dynamic correlation. Spin–orbit coupling perturbation was considered with the QDPT (quasi-degenerate perturbation theory) approach. Spin–spin couplings have been neglected as they are very small and incorrectly estimated through the CASSCF method. Final spin-Hamiltonian parameters were computed with the universal effective Hamiltonian approach (EHA).³³

Additionally, CASSCF-RASSI-SO calculations have also been performed by using the MOLCAS 8.0 program.³⁴ For this relativistic contracted ANO-type orbitals were used from basis library ANO-RCC...6s5p3d2f1g for Co, ANO-RCC...5s4p2d1f for diamagnetic counterpart Zn; ANO-RCC...4s3p2d for N and O; ANO-RCC...5s4p2d for Cl; ANO-RCC...4s3p1d for S; ANO-RCC...6s5p3d for Br; ANO-RCC...6s5p3d1f for I; ANO-RCC...3s2p for C; and ANO-RCC...2s for H. The Douglas–Kroll–Hess (DKH) Hamiltonian was employed during the calculations to account for the scalar relativistic effect. In the configuration step similar roots, i.e., seven electrons in five Co d-orbitals, were used and optimized with 10 quartets and 40 doublets. These states were allowed to mix and interacted in the RASSI (restricted active space state interaction) step, and subsequent spin–orbit (SO) coupling was also introduced in this RASSI step. Local spin-Hamiltonian parameters like *D*, *E/D*, and *g*-factors have been computed by using the SINGLE_ANISO module from the EHA method.³² These were finally used to compute anisotropic exchange parameter *J* by using the POLY_ANISO module.³⁵

■ ASSOCIATED CONTENT

Supporting Information

The Supporting Information is available free of charge at <https://pubs.acs.org/doi/10.1021/acs.inorgchem.1c00956>.

PXRD, plots, and additional data of magnetic characterizations (PDF)

Accession Codes

CCDC 1970738–1970741 contain the supplementary crystallographic data for this paper. These data can be obtained free of charge via www.ccdc.cam.ac.uk/data_request/cif, or by emailing data_request@ccdc.cam.ac.uk, or by contacting The Cambridge Crystallographic Data Centre, 12 Union Road, Cambridge CB2 1EZ, UK; fax: +44 1223 336033.

■ AUTHOR INFORMATION

Corresponding Authors

Sanjit Konar – Department of Chemistry, Indian Institute of Science Education and Research (IISER), Bhopal, Bhopal

462066, India; orcid.org/0000-0002-1584-6258;

Phone: +91-755-6691313; Email: skonar@iiserb.ac.in

Gopalan Rajaraman – Department of Chemistry, Indian Institute of Technology, Bombay, Mumbai 400076, India;

orcid.org/0000-0001-6133-3026; Email: rajaraman@chem.iitb.ac.in

Authors

Ajit Kumar Kharwar – Department of Chemistry, Indian Institute of Science Education and Research (IISER), Bhopal, Bhopal 462066, India

Arpan Mondal – Department of Chemistry, Indian Institute of Science Education and Research (IISER), Bhopal, Bhopal 462066, India; orcid.org/0000-0001-9192-7255

Arup Sarkar – Department of Chemistry, Indian Institute of Technology, Bombay, Mumbai 400076, India

Complete contact information is available at:

<https://pubs.acs.org/doi/10.1021/acs.inorgchem.1c00956>

Author Contributions

[§]A.K.K. and A.M. contributed equally to this work.

Notes

The authors declare no competing financial interest.

■ ACKNOWLEDGMENTS

A.K.K.H. acknowledges CSIR for a SRF fellowship. A.S. thanks IIT Bombay for IPDF funding. A.M. thanks IISER Bhopal for SRF fellowship. S.K. thanks CSIR (Project no. 01(2974)/19/EMR-II) and SERB (Project no. CRG/2018/000072), Government of India, for financial support. G.R. thanks DST and SERB for funding (CRG/2018/000430; DST/SJF/CSA-03/2018-10; SB/SJF/2019-20/12).

■ REFERENCES

- (1) (a) Rinehart, J. D.; Fang, M.; Evans, W. J.; Long, J. R. A N23–Radical-Bridged Terbium Complex Exhibiting Magnetic Hysteresis at 14 K. *J. Am. Chem. Soc.* **2011**, *133* (36), 14236. (b) Singh, S. K.; Beg, M. F.; Rajaraman, G. Role of Magnetic Exchange Interactions in the Magnetization Relaxation of {3d–4f} Single-Molecule Magnets: A Theoretical Perspective. *Chem. - Eur. J.* **2016**, *22* (2), 672. (c) Goswami, S.; Mondal, A. K.; Konar, S. Nanoscopic molecular magnets. *Inorg. Chem. Front.* **2015**, *2* (8), 687.
- (2) (a) Shi, W.; Chen, X.-Y.; Zhao, B.; Yu, A.; Song, H.-B.; Cheng, P.; Wang, H.-G.; Liao, D.-Z.; Yan, S.-P. Construction of 3d–4f Mixed-Metal Complexes Based on a Binuclear Oxovanadium Unit: Synthesis, Crystal Structure, EPR, and Magnetic Properties. *Inorg. Chem.* **2006**, *45* (10), 3949. (b) Zhang, J.-J.; Hu, S.-M.; Xiang, S.-C.; Sheng, T.; Wu, X.-T.; Li, Y.-M. Syntheses, Structures, and Properties of High-Nuclear 3d–4f Clusters with Amino Acid as Ligand: {Gd₆Cu₂₄}, {Tb₆Cu₂₆}, and {(Ln₆Cu₂₄)₂Cu} (Ln = Sm, Gd). *Inorg. Chem.* **2006**, *45* (18), 7173. (c) Sharples, J. W.; Collison, D. The coordination chemistry and magnetism of some 3d–4f and 4f amino-polyalcohol compounds. *Coord. Chem. Rev.* **2014**, *260*, 1.
- (3) (a) Li, X.-L.; Min, F.-Y.; Wang, C.; Lin, S.-Y.; Liu, Z.; Tang, J. Utilizing 3d–4f Magnetic Interaction to Slow the Magnetic Relaxation of Heterometallic Complexes. *Inorg. Chem.* **2015**, *54* (9), 4337. (b) Feltham, H. L. C.; Clérac, R.; Powell, A. K.; Brooker, S. A Tetranuclear, Macrocyclic 3d–4f Complex Showing Single-Molecule Magnet Behavior. *Inorg. Chem.* **2011**, *50* (10), 4232. (c) Mishra, A.; Wernsdorfer, W.; Parsons, S.; Christou, G.; Brechin, E. K. The search for 3d–4f single-molecule magnets: synthesis, structure and magnetic properties of a [Mn^{III}₂Dy^{III}₂] cluster. *Chem. Commun.* **2005**, *16*, 2086–2088. (d) Collet, A.; Wilson, C.; Murrie, M. Microwave-assisted synthesis: from a mononuclear {Co^{II}} complex to {Co^{II}} solvomorphs. *Dalton Trans.* **2019**, *48* (3), 854.

- (4) (a) Barros, W. P.; Inglis, R.; Nichol, G. S.; Rajeshkumar, T.; Rajaraman, G.; Piligkos, S.; Stumpf, H. O.; Brechin, E. K. From antiferromagnetic to ferromagnetic exchange in a family of oxime-based Mn^{III} dimers: a magneto-structural study. *Dalton Trans.* **2013**, 42 (47), 16510. (b) Berg, N.; Rajeshkumar, T.; Taylor, S. M.; Brechin, E. K.; Rajaraman, G.; Jones, L. F. What Controls the Magnetic Interaction in bis- μ -Alkoxo Mn^{III} Dimers? A Combined Experimental and Theoretical Exploration. *Chem. - Eur. J.* **2012**, 18 (19), 5906. (c) Sheikh, J. A.; Jena, H. S.; Clearfield, A.; Konar, S. Phosphonate Based High Nuclearity Magnetic Cages. *Acc. Chem. Res.* **2016**, 49 (6), 1093. (d) Khanra, S.; Konar, S.; Clearfield, A.; Helliwell, M.; McInnes, E. J. L.; Tolis, E.; Tuna, F.; Winpenny, R. E. P. Synthesis, Structural and Magnetochemical Studies of Iron Phosphonate Cages Based on {Fe₃O}⁷⁺ Core. *Inorg. Chem.* **2009**, 48 (12), 5338. (e) Adhikary, A.; Sheikh, J. A.; Biswas, S.; Konar, S. Synthesis, crystal structure and study of magnetocaloric effect and single molecular magnetic behaviour in discrete lanthanide complexes. *Dalton Trans.* **2014**, 43 (24), 9334. (f) Kharwar, A. K.; Konar, S. Exchange coupled Co(II) based layered and porous metal-organic frameworks: structural diversity, gas adsorption, and magnetic properties. *Dalton Trans.* **2020**, 49 (13), 4012. (g) Adams, H.; Bradshaw, D.; Fenton, D. E. Dinuclear Zinc(II) Complexes of N,N'-Bis[2-(hydroxyphenyl)methyl]-N,N'-bis(2-pyridylmethyl)-1, n-alkane-diamines. *Eur. J. Inorg. Chem.* **2001**, 2001 (3), 859–864.
- (5) (a) Kahn, O. Dinuclear Complexes with Predictable Magnetic Properties. *Angew. Chem., Int. Ed. Engl.* **1985**, 24 (10), 834. (b) Pei, Y.; Verdaguier, M.; Kahn, O.; Sletten, J.; Renard, J. P. Ferromagnetic transition in a bimetallic molecular system. *J. Am. Chem. Soc.* **1986**, 108 (23), 7428.
- (6) Guha, B. C.; Penney, W. G. Magnetic properties of some paramagnetic crystals at low temperatures. *Proc. R. Soc. London. Ser. A* **1951**, 206 (1086), 353.
- (7) Bleaney, B.; Bowers, K. D. Anomalous paramagnetism of copper acetate. *Proc. R. Soc. London. Ser. A* **1952**, 214 (1119), 451.
- (8) Leising, R. A.; Kim, J.; Perez, M. A.; Que, L. Alkane functionalization at (μ -oxo)diiron(III) centers. *J. Am. Chem. Soc.* **1993**, 115 (21), 9524.
- (9) (a) Robertson, N. J.; Carney, M. J.; Halfen, J. A. Chromium(II) and Chromium(III) Complexes Supported by Tris(2-pyridylmethyl)-amine: Synthesis, Structures, and Reactivity. *Inorg. Chem.* **2003**, 42 (21), 6876. (b) Hodgson, D. J.; Zietlow, M. H.; Pedersen, E.; Toftlund, H. Synthesis and magnetic and structural characterization of the binuclear complex di- μ -hydroxobis{[tris(2-pyridylmethyl)amine]-chromium(III)} perchlorate tetrahydrate, [(tpa)CrOH]₂(ClO₄)₄·4H₂O. *Inorg. Chim. Acta* **1988**, 149 (1), 111. (c) Gafford, B. G.; Holwerda, R. A. Oxidative synthesis of bis(μ -hydroxo)chromium(III) dimers with aromatic amine ligands. Structure, physical properties, and base hydrolysis kinetics of the bis(μ -hydroxo)bis[tris(2-pyridylmethyl)amine]chromium(III) ion. *Inorg. Chem.* **1989**, 28 (1), 60. (d) Gafford, B. G.; Marsh, R. E.; Schaefer, W. P.; Zhang, J. H.; O'Connor, C. J.; Holwerda, R. A. Synthesis, structure and physical properties of (μ -oxo)(μ -carboxylato)bis{tris(2-pyridylmethyl)amine}chromium(III) complexes. *Inorg. Chem.* **1990**, 29 (23), 4652.
- (10) (a) Towle, D. K.; Botsford, C. A.; Hodgson, D. J. Synthesis and characterization of the binuclear mixed valence complex di- μ -oxobis[tris(2-methyl-pyridyl)amine] dimanganese(III, IV) dithionate heptahydrate, [(tpa)MnO]₂(S₂O₆)_{3/2}·7H₂O. *Inorg. Chim. Acta* **1988**, 141 (2), 167. (b) Shin, B.-K.; Kim, Y.; Kim, M.; Han, J. Synthesis, structure and catalase activity of the [TPA₂Mn₂(μ -Cl)₂]²⁺ complex. *Polyhedron* **2007**, 26 (15), 4557.
- (11) Tong, B.; Chang, S.-C.; Carpenter, E. E.; O'Connor, C. J.; Lay Jr, J. O.; Norman, R. E. Di- μ -halo-bis{[tris(2-pyridylmethyl)amine- κ 4N]nickel(II)} bis(triethylammonium) tetraperchlorate: Magneto-structural studies. *Inorg. Chim. Acta* **2000**, 300–302, 855.
- (12) Pantazis, D. A.; Krewald, V.; Orto, M.; Neese, F. Theoretical magnetochemistry of dinuclear manganese complexes: broken symmetry density functional theory investigation on the influence of bridging motifs on structure and magnetism. *Dalton Trans.* **2010**, 39 (20), 4959.
- (13) (a) Roy Chowdhury, S.; Mishra, S. Large Magnetic Anisotropy in Linear CoII Complexes – Ab Initio Investigation of the Roles of Ligand Field, Structural Distortion, and Conformational Dynamics. *Eur. J. Inorg. Chem.* **2017**, 659. (b) Meng, Y.-S.; Jiang, S.-D.; Wang, B.-W.; Gao, S. Understanding the Magnetic Anisotropy toward Single-Ion Magnets. *Acc. Chem. Res.* **2016**, 49 (11), 2381. (c) Murrie, M. Cobalt(II) single-molecule magnets. *Chem. Soc. Rev.* **2010**, 39 (6), 1986. (d) Ostrovsky, S.; Tomkiewicz, Z.; Haase, W. High-spin Co(II) in monomeric and exchange coupled oligomeric structures: Magnetic and magnetic circular dichroism investigations. *Coord. Chem. Rev.* **2009**, 253 (19), 2363.
- (14) (a) Rechkemmer, Y.; Breitgoff, F. D.; van der Meer, M.; Atanasov, M.; Hakl, M.; Orlita, M.; Neugebauer, P.; Neese, F.; Sarkar, B.; van Slageren, J. A four-coordinate cobalt(II) single-ion magnet with coercivity and a very high energy barrier. *Nat. Commun.* **2016**, 7 (1), 10467. (b) Świtlicka, A.; Machura, B.; Penkala, M.; Bińko, A.; Bińko, D. C.; Titiš, J.; Rajnák, C.; Boča, R.; Ozarowski, A.; Ozerov, M. Slow Magnetic Relaxation in Cobalt(II) Field-Induced Single-Ion Magnets with Positive Large Anisotropy. *Inorg. Chem.* **2018**, 57 (20), 12740. (c) Böhme, M.; Ziegenbalg, S.; Aliabadi, A.; Schnegg, A.; Görls, H.; Plass, W. Magnetic relaxation in cobalt(II)-based single-ion magnets influenced by distortion of the pseudotetrahedral [N2O2] coordination environment. *Dalton Trans.* **2018**, 47 (32), 10861. (d) Galloway, K. W.; Whyte, A. M.; Wernsdorfer, W.; Sanchez-Benitez, J.; Kamenev, K. V.; Parkin, A.; Peacock, R. D.; Murrie, M. Cobalt(II) Citrate Cubane Single-Molecule Magnet. *Inorg. Chem.* **2008**, 47 (16), 7438.
- (15) (a) Vallejo, J.; Fortea-Pérez, F. R.; Pardo, E.; Benmansour, S.; Castro, I.; Krzystek, J.; Armentano, D.; Cano, J. Guest-dependent single-ion magnet behaviour in a cobalt(ii) metal-organic framework. *Chem. Sci.* **2016**, 7 (3), 2286. (b) Shao, D.; Shi, L.; Wei, H.-Y.; Wang, X.-Y. Field-Induced Single-Ion Magnet Behaviour in Two New Cobalt(II) Coordination Polymers with 2,4,6-Tris(4-pyridyl)-1,3,5-triazine. *Inorganics* **2017**, 5 (4), 90. (c) Guedes, G. P.; Soriano, S.; Comerlato, N. M.; Speziali, N. L.; Novak, M. A.; Vaz, M. G. F. Heptanuclear cobalt(II) dicubane compounds with single-molecule magnet behavior. *Inorg. Chem. Commun.* **2013**, 37, 101.
- (16) (a) Mondal, A. K.; Goswami, T.; Misra, A.; Konar, S. Probing the Effects of Ligand Field and Coordination Geometry on Magnetic Anisotropy of Pentacoordinate Cobalt(II) Single-Ion Magnets. *Inorg. Chem.* **2017**, 56 (12), 6870. (b) Mondal, A. K.; Sundararajan, M.; Konar, S. A new series of tetrahedral Co(II) complexes [CoLX₂] (X = NCS, Cl, Br, I) manifesting single-ion magnet features. *Dalton Trans.* **2018**, 47 (11), 3745. (c) Mondal, A. K.; Jover, J.; Ruiz, E.; Konar, S. Investigation of easy-plane magnetic anisotropy in P-ligand square-pyramidal Co^{II} single ion magnets. *Chem. Commun.* **2017**, 53 (38), 5338. (d) Khatua, S.; Goswami, S.; Parshamoni, S.; Jena, H. S.; Konar, S. A 2D coordination polymer based on Co3-SBU showing spin-canting ferromagnetic behaviour. *RSC Adv.* **2013**, 3 (47), 25237. (e) Mondal, A. K.; Khatua, S.; Tomar, K.; Konar, S. Field-Induced Single-Ion-Magnetic Behavior of Octahedral Co^{II} in a Two-Dimensional Coordination Polymer. *Eur. J. Inorg. Chem.* **2016**, 2016 (22), 3545. (f) Mondal, P.; Dey, B.; Roy, S.; Bera, S. P.; Nasani, R.; Santra, A.; Konar, S. Field-Induced Slow Magnetic Relaxation and Anion/Solvent Dependent Proton Conduction in Cobalt(II) Coordination Polymers. *Cryst. Growth Des.* **2018**, 18 (10), 6211. (g) Mondal, A.; Kharwar, A. K.; Konar, S. Sizeable Effect of Lattice Solvent on Field Induced Slow Magnetic Relaxation in Seven Coordinated CoII Complexes. *Inorg. Chem.* **2019**, 58 (16), 10686.
- (17) (a) Mondal, A. K.; Parmar, V. S.; Biswas, S.; Konar, S. Tetrahedral M^{II} based binuclear double-stranded helicates: single-ion-magnet and fluorescence behaviour. *Dalton Trans.* **2016**, 45 (11), 4548. (b) Kharwar, A. K.; Mondal, A.; Konar, S. Alignment of axial anisotropy of a mononuclear hexa-coordinated Co(II) complex in a lattice shows improved single molecule magnetic behavior over a 2D coordination polymer having a similar ligand field. *Dalton Trans.* **2021**, 50 (8), 2832.
- (18) (a) Sakiyama, H.; Ito, R.; Kumagai, H.; Inoue, K.; Sakamoto, M.; Nishida, Y.; Yamasaki, M. Dinuclear Cobalt(II) Complexes of an

Acyclic Phenol-Based Dinucleating Ligand with Four Methoxyethyl Chelating Arms – First Magnetic Analyses in an Axially Distorted Octahedral Field. *Eur. J. Inorg. Chem.* **2001**, 2001 (8), 2027. (b) Carbonera, C.; Dei, A.; Létard, J.-F.; Sangregorio, C.; Sorace, L. Thermally and Light-Induced Valence Tautomeric Transition in a Dinuclear Cobalt–Tetraoxolene Complex. *Angew. Chem., Int. Ed.* **2004**, 43 (24), 3136. (c) El-Khatib, F.; Cahier, B.; Shao, F.; López-Jordà, M.; Guillot, R.; Rivière, E.; Hafez, H.; Saad, Z.; Girerd, J.-J.; Guihéry, N.; Mallah, T. Design and Magnetic Properties of a Mononuclear Co(II) Single Molecule Magnet and Its Antiferromagnetically Coupled Binuclear Derivative. *Inorg. Chem.* **2017**, 56 (8), 4601–4608.

(19) Kong, J.-J.; Jiang, Y.-X.; Zhang, J.-C.; Shao, D.; Huang, X.-C. Two-dimensional magnetic materials of cobalt(II) triangular lattices constructed by a mixed benzimidazole–dicarboxylate strategy. *CrystEngComm* **2019**, 21 (15), 2596.

(20) Alvarez, S.; Alemany, P.; Casanova, D.; Cirera, J.; Llunell, M.; Avnir, D. Shape Maps and Polyhedral Interconversion Paths in Transition Metal Chemistry. *Coord. Chem. Rev.* **2005**, 249, 1693.

(21) Chilton, N. F.; Anderson, R. P.; Turner, L. D.; Soncini, A.; Murray, K. S. PHI: A powerful new program for the analysis of anisotropic monomeric and exchange-coupled polynuclear d- and f-block complexes. *J. Comput. Chem.* **2013**, 34 (13), 1164.

(22) (a) Black, D.; Blake, A. J.; Dancy, K. P.; Harrison, A.; McPartlin, M.; Parsons, S.; Tasker, P. A.; Whittaker, G.; Schroder, M. Synthesis, structures and magnetochemistry of binuclear cobalt(II), nickel(II) and copper(II) complexes of 2,6-diformyl-4-methylphenol dioxime. *J. Chem. Soc., Dalton Trans.* **1998**, 23, 3953. (b) Tone, K.; Sakiyama, H.; Mikuriya, M.; Yamasaki, M.; Nishida, Y. Magnetic behavior of dinuclear cobalt(II) complexes assumed to be caused by a paramagnetic impurity can be explained by tilts of local distortion axes. *Inorg. Chem. Commun.* **2007**, 10 (8), 944. (c) Hossain, M. J.; Yamasaki, M.; Mikuriya, M.; Kuribayashi, A.; Sakiyama, H. Synthesis, Structure, and Magnetic Properties of Dinuclear Cobalt(II) Complexes with a New Phenol-Based Dinucleating Ligand with Four Hydroxyethyl Chelating Arms. *Inorg. Chem.* **2002**, 41 (15), 4058. (d) Mukherjee, A.; Lloret, F.; Mukherjee, R. Synthesis and Properties of Diphenoxo-Bridged Co^{II}, Ni^{II}, Cu^{II}, and Zn^{II} Complexes of a New Tripodal Ligand: Generation and Properties of M^{II}-Coordinated Phenoxyl Radical Species. *Inorg. Chem.* **2008**, 47 (11), 4471. (e) Massoud, S. S.; Spell, M.; Ledet, C. C.; Junk, T.; Herchel, R.; Fischer, R. C.; Trávníček, Z.; Mautner, F. A. Magnetic and structural properties of dinuclear singly bridged-phenoxido metal(II) complexes. *Dalton Trans.* **2015**, 44 (5), 2110. (f) Lin, S.-Y.; Xu, G.-F.; Zhao, L.; Tang, J.; Liu, G.-X. Structure and Magnetic Properties of a μ -Phenoxido-bridged Dinuclear Cobalt(II) Complex. *Z. Anorg. Allg. Chem.* **2011**, 637 (6), 720. (g) Liu, J.-J.; Jiang, S.-D.; Neugebauer, P.; van Slageren, J.; Lan, Y.; Wernsdorfer, W.; Wang, B.-W.; Gao, S. Magnetic and HFEP studies of Exchange Coupling in a Series of μ -Cl Dicobalt Complexes. *Inorg. Chem.* **2017**, 56 (5), 2417.

(23) (a) Suturina, E. A.; Maganas, D.; Bill, E.; Atanasov, M.; Neese, F. Magneto-Structural Correlations in a Series of Pseudotetrahedral [Co^{II}(XR)₄]²⁻ Single Molecule Magnets: An ab Initio Ligand Field Study. *Inorg. Chem.* **2015**, 54 (20), 9948. (b) Sarkar, A.; Tewary, S.; Sinkar, S.; Rajaraman, G. Magnetic Anisotropy in Co^{II}X₄ (X = O, S, Se) Single-Ion Magnets: Role of Structural Distortions versus Heavy Atom Effect. *Chem. - Asian J.* **2019**, 14 (24), 4696.

(24) (a) Zhu, Y.-Y.; Cui, C.; Zhang, Y.-Q.; Jia, J.-H.; Guo, X.; Gao, C.; Qian, K.; Jiang, S.-D.; Wang, B.-W.; Wang, Z.-M.; et al. Zero-field slow magnetic relaxation from single Co(II) ion: a transition metal single-molecule magnet with high anisotropy barrier. *Chem. Sci.* **2013**, 4 (4), 1802. (b) Novikov, V. V.; Pavlov, A. A.; Nelyubina, Y. V.; Boulon, M.-E.; Varzatskii, O. A.; Voloshin, Y. Z.; Winpenny, R. E. P. A Trigonal Prismatic Mononuclear Cobalt(II) Complex Showing Single-Molecule Magnet Behavior. *J. Am. Chem. Soc.* **2015**, 137 (31), 9792. (c) Zhu, Y.-Y.; Zhang, Y.-Q.; Yin, T.-T.; Gao, C.; Wang, B.-W.; Gao, S. A Family of CoIICoIII3 Single-Ion Magnets with Zero-Field Slow Magnetic Relaxation: Fine Tuning of Energy Barrier by Remote Substituent and Counter Cation. *Inorg. Chem.* **2015**, 54 (11),

5475. (d) Pavlov, A. A.; Nelyubina, Y. V.; Kats, S. V.; Penkova, L. V.; Efimov, N. N.; Dmitrienko, A. O.; Vologzhanina, A. V.; Belov, A. S.; Voloshin, Y. Z.; Novikov, V. V. Polymorphism in a Cobalt-Based Single-Ion Magnet Tuning Its Barrier to Magnetization Relaxation. *J. Phys. Chem. Lett.* **2016**, 7 (20), 4111. (e) Peng, Y.; Bodenstein, T.; Fink, K.; Mereacre, V.; Anson, C. E.; Powell, A. K. Magnetic anisotropy of a Co^{II} single ion magnet with distorted trigonal prismatic coordination: theory and experiment. *Phys. Chem. Chem. Phys.* **2016**, 18 (43), 30135. (f) Zhang, Y.-Z.; Gómez-Coca, S.; Brown, A. J.; Saber, M. R.; Zhang, X.; Dunbar, K. R. Trigonal antiprismatic Co(II) single molecule magnets with large uniaxial anisotropies: importance of Raman and tunneling mechanisms. *Chem. Sci.* **2016**, 7 (10), 6519. (g) Ozumerzifon, T. J.; Bhowmik, I.; Spaller, W. C.; Rappé, A. K.; Shores, M. P. Toward steric control of guest binding modality: a cationic Co(II) complex exhibiting cation binding and zero-field relaxation. *Chem. Commun.* **2017**, 53 (30), 4211. (h) Sarkar, A.; Dey, S.; Rajaraman, G. Role of Coordination Number and Geometry in Controlling the Magnetic Anisotropy in Fe^{II}, Co^{II}, and Ni^{II} Single-Ion Magnets. *Chem. - Eur. J.* **2020**, 26 (62), 14036–14058.

(25) Ruamps, R.; Maurice, R.; Batchelor, L.; Boggio-Pasqua, M.; Guillot, R.; Barra, A. L.; Liu, J.; Bendeif, E.-E.; Pillet, S.; Hill, S.; et al. Giant Ising-Type Magnetic Anisotropy in Trigonal Bipyramidal Ni(II) Complexes: Experiment and Theory. *J. Am. Chem. Soc.* **2013**, 135 (8), 3017.

(26) (a) Vaidya, S.; Upadhyay, A.; Singh, S. K.; Gupta, T.; Tewary, S.; Langley, S. K.; Walsh, J. P. S.; Murray, K. S.; Rajaraman, G.; Shanmugam, M. A synthetic strategy for switching the single ion anisotropy in tetrahedral Co(II) complexes. *Chem. Commun.* **2015**, 51 (18), 3739. (b) Vaidya, S.; Singh, S. K.; Shukla, P.; Ansari, K.; Rajaraman, G.; Shanmugam, M. Role of Halide Ions in the Nature of the Magnetic Anisotropy in Tetrahedral Co^{II} Complexes. *Chem. - Eur. J.* **2017**, 23 (40), 9546.

(27) Chibotaru, L. F.; Ungur, L.; Aronica, C.; Elmoll, H.; Pilet, G.; Luneau, D. Structure, Magnetism, and Theoretical Study of a Mixed-Valence Co^{III}₃Co^{II}₄ Heptanuclear Wheel: Lack of SMM Behavior despite Negative Magnetic Anisotropy. *J. Am. Chem. Soc.* **2008**, 130 (37), 12445.

(28) Kahn, O. *Molecular Magnetism*, VCH Publishers, Inc.: 1993

(29) Dolomanov, O. V.; Bourhis, L. J.; Gildea, R. J.; Howard, J. A. K.; Puschmann, H. OLEX2: a complete structure solution, refinement and analysis program. *J. Appl. Crystallogr.* **2009**, 42 (2), 339.

(30) Sheldrick, G. Crystal structure refinement with SHELXL. *Acta Crystallogr., Sect. C: Struct. Chem.* **2015**, 71 (1), 3.

(31) Liu, J.; Chen, Y.-C.; Liu, J.-L.; Vieru, V.; Ungur, L.; Jia, J.-H.; Chibotaru, L. F.; Lan, Y.; Wernsdorfer, W.; Gao, S.; et al. A Stable Pentagonal Bipyramidal Dy(III) Single-Ion Magnet with a Record Magnetization Reversal Barrier over 1000 K. *J. Am. Chem. Soc.* **2016**, 138 (16), 5441.

(32) Neese, F. Software update: the ORCA program system, version 4.0. *Wiley Interdiscip. Rev.: Comput. Mol. Sci.* **2018**, 8 (1), e1327.

(33) Maurice, R.; Bastardis, R.; Graaf, C. d.; Suaud, N.; Mallah, T.; Guihéry, N. Universal Theoretical Approach to Extract Anisotropic Spin Hamiltonians. *J. Chem. Theory Comput.* **2009**, 5 (11), 2977.

(34) Aquilante, F.; Autschbach, J.; Carlson, R. K.; Chibotaru, L. F.; Delcey, M. G.; De Vico, L.; Fdez. Galván, I.; Ferré, N.; Frutos, L. M.; Gagliardi, L.; et al. Molcas 8: New capabilities for multiconfigurational quantum chemical calculations across the periodic table. *J. Comput. Chem.* **2016**, 37 (5), 506.

(35) Chibotaru, L. F.; Ungur, L.; Soncini, A. The Origin of Nonmagnetic Kramers Doublets in the Ground State of Dysprosium Triangles: Evidence for a Toroidal Magnetic Moment. *Angew. Chem., Int. Ed.* **2008**, 47 (22), 4126.